GEOPHYSICAL RESEARCH LETTERS, VOL. 22, NO. 5, PAGES 531-534, MARCH 1, 1995

Direct evidence for the undulation of the 660-km discontinuity beneath Tonga: Comparison of Japan and California array data

Fenglin Niu and Hitoshi Kawakatsu

Earthquake Research Institute, University of Tokyo

Abstract. Short-period seismograms of Tonga deep earthquakes recorded by Japanese and Californian seismic networks are stacked to identify the S-P converted wave associated with the 660-km discontinuity. The travel-time difference between this S-P converted wave and the direct P wave is used to constrain the depth of the 660-km discontinuity. Analysis of a total of 29 events produced a detailed topographical map of the discontinuity beneath the Tonga subduction zone. Two events which exhibit clear S-P conversions in both Japan and California data are selected to show directly the depth variations of the 660-km discontinuity adjacent to the subducting slab. The S-P conversion points on the ray paths to Japan are observed to be approximately 10 to 30 km deeper than the conversion points on those to California, which represents direct evidence for a slab-induced depression of the 660-km discontinuity.

Introduction

Seismic constraints on depth variations of the 660-km discontinuity adjacent to subducting slabs can play a key role in our understanding of the physical nature of the discontinuity. The 660-km discontinuity may represent either a compositional boundary or a phase transition. High-pressure experiments indicate that the upper mantle mineral assemblage (primary γ-spinel) transforms to perovskite plus magnesiowustite, which are generally believed to represent the primary constituents of the lower mantle, at the approximate pressure-temperature conditions believed to occur at a depth of 660 km [*Ito and Takahashi*, 1989]. An approximately 20 $\sim$ 60 km depression of this transitional boundary is anticipated within the cold interior of subducted slabs, depending the Clapeyron slope of the endothermic γ-spinel to perovskite transition. On the other hand, dynamic models predict that a chemical boundary may be depressed by as much as 100 to 300 km [*Kincaid and Olson*, 1987]. Seismic observations may be able to tell us which of these contending explanations is more realistic.

Short-period S-P conversion phases at the 660-km discontinuity are often used to constrain the depth of the discontinuity within the slab [e.g. *Bock and Ha*, 1984; *Richards and Wicks*, 1990; *Mizuta et al.*, 1991; *Vidale and Benz*, 1992; *Wicks and Richards*, 1993]. *Wicks and Richards* [1993] observed a maximum 60-km slab-induced depression beneath the Izu-Bonin arc using data from the Warramunga Seismic Array in Australia; *Vidale and Benz* [1992] obtained a depth perturbation of less than 30 km beneath several subduction zones using data for 6 deep earthquakes collected from Californian regional arrays; *Shearer and Masters* [1992] reported a 20 km deep trough beneath Kuril-Kamchatka from long-period SS precursors.

In this paper we use a large number of teleseismic seismograms from Japanese and Californian arrays for 29 deep events that occurred in the Tonga subduction zone to constrain the depth variations of the 660-km discontinuity adjacent to the subducting slab. We further introduce a direct comparison of Japanese data with Californian data from some of those events to reduce the uncertainties (i.e., effect of source mislocation, high velocity slab, etc.) in determining the depth of the 660-km discontinuity and confirm the existence of a depression of the discontinuity.

Data and Analysis

The Japanese array used in this study is the J-array [*J-array Group*, 1993] which is comprised of numerous local seismic networks operated by various Japanese national universities and research institutes. It covers the entirety of the Japanese islands with more than 300 high-quality short-period (1 Hz) vertical-component seismographs. In an effort to compensate for the relatively small amount of data accumulated by the J-array since April 1991, we also use short period seismograms from the Southern California Seismic Network (SCSN; hereafter referred to as the California array). The California array consists of more than 300 stations within a radius of approximately 500 km and has accumulated a large quantity of data since 1981.

We analyze a total of 29 deep events with a magnitude between 5.9 and 6.9 that occurred in the Tonga subduction zone since 1984 (Table 1). Nine of these were recorded by the J-array (for two events that occurred before the operation of the J-array we utilize the data of the regional network of the Earthquake Research Institute of the University of Tokyo, which is located in central Japan) and twenty-six by the California array. We redetermine the hypocentral depths by fitting the observed pP-P travel-time difference obtained

Paper number 94GL03332
0094-8534/95/94GL-03332$03.00

Table 1. Earthquakes

Date (yr mo d)	Time (h min s)	Lon.	Lat.	Depth PDE	pP-P	Mag. Mw	'660'depth (JP	US)*
1984 01 19	16 15 16.7	181.63	-23.63	335.7	327.	6.2	-	665.
1984 04 22	03 33 00.7	180.58	-21.83	616.6	595.	6.3	-	675.
1984 04 25	04 19 31.9	182.77	-17.29	418.4	406.	6.3	-	†
1984 08 26	05 00 45.8	179.07	-23.57	571.8	572.	6.4	-	670.
1984 09 28	03 03 50.9	182.02	-21.42	384.6	370.	6.0	-	665.
1984 11 15	05 52 30.3	182.54	-20.36	305.3	340.	6.3	-	660.
1984 11 17	13 45 49.1	181.91	-18.74	471.5	455.	6.7	-	665.
1984 11 22	17 07 36.4	181.91	-17.77	663.0	650.	6.5	-	700.
1985 08 28	20 50 48.4	180.99	-21.01	640.4	628.	6.6	-	705.
1986 04 01	10 13 41.2	181.37	-17.91	562.4	545.	5.9	-	670.
1986 05 26	18 40 46.1	180.74	-21.72	603.4	597.	6.8	-	665.
1987 02 10	00 59 29.3	182.52	-19.45	418.5	397.	6.4	-	†
1987 04 29	14 27 36.6	182.14	-18.93	410.6	395.	6.5	-	655.
1988 03 10	10 25 04.8	181.30	-20.88	635.9	632.	6.6	-	685.
1989 04 30	15 33 52.9	181.25	-17.82	591.2	572.	6.0	-	†
1989 10 23	13 08 25.5	179.79	-25.56	480.3	451.	6.1	-	655.
1989 11 16	08 39 42.3	180.94	-17.69	555.1	530.	6.2	-	660.
1989 11 29	05 49 03.4	179.52	-25.39	515.6	505.	6.1	-	665.
1990 06 08	15 05 10.3	181.10	-18.70	499.0	518.	6.4	660.	-
1990 07 11	19 48 09.5	178.22	-25.22	596.4	591.	6.0	-	†
1990 07 22	09 26 18.0	179.93	-23.48	531.0	535.	6.3	660.	655.
1990 10 10	05 54 58.0	178.87	-23.35	575.1	559.	6.0	-	†
1991 06 09	07 45 06.6	183.69	-20.18	278.0	287.	6.9	660.	†
1991 09 30	00 21 47.5	181.41	-20.88	579.0	595.	6.9	685.	675.
1991 12 03	10 33 42.0	178.57	-26.31	561.0	559.	6.3	730.	700.
1992 08 30	10 33 42.0	181.23	-17.74	574.0	565.	6.4	710.	†
1992 11 12	22 28 58.4	181.92	-22.35	368.0	375.	6.2	655.	†
1993 04 16	14 08 40.0	181.10	-17.40	569.0	563.	6.9	670.	†
1993 08 07	17 53 28.5	179.10	-23.60	560.0	553.	6.7	710.	700.

* JP: J-Array; US: California Array
- : No Array data; †: No observed $S_{660}P$

from J-array data and broadband data from globally distributed IRIS stations. Source parameters and relevant array data are listed in Table 1.

Seismograms with favorable signal-to-noise ratios are selected and low passed at a corner period of 2 sec. The seismograms are subsequently aligned so that the maximum amplitude, which is normalized to unity, occurs at time zero. The polarity of the seismogram is also reversed when necessary. We employ a time window of 150-s for the J-array data. In the case of the California array data, a shorter time window, usually the maximum time length of the record (30 ~ 50 sec), is used. Approximately 40 to 120 station records are selected for an N-th root stacking process [e.g., *Kanasewich*, 1973; *Vidale and Benz*, 1992; *Richards and Wicks*, 1990]; here, we use $N = 2$. Fig. 1 shows a representative result of the N-th root stack; black clusters represent greater

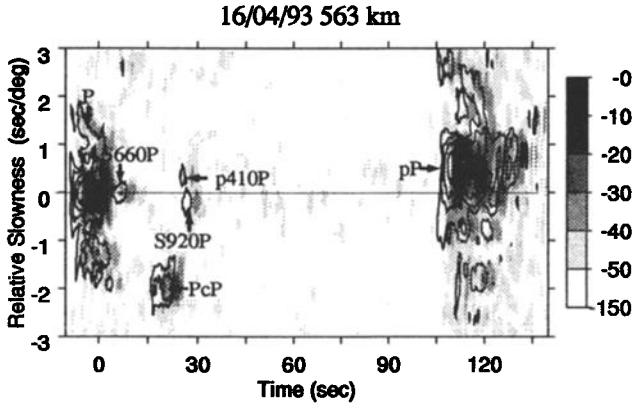

Fig. 1 N-th root stacked waveforms in which normalized amplitudes are plotted as a function of relative slowness with respect to the direct P wave *vs.* arrival time (see text). Note that later phases, which are ambiguous in individual seismogram (not shown), are clearly evident in the stacked data. Also, note the slight difference in slowness between the direct P-wave and the later phases.

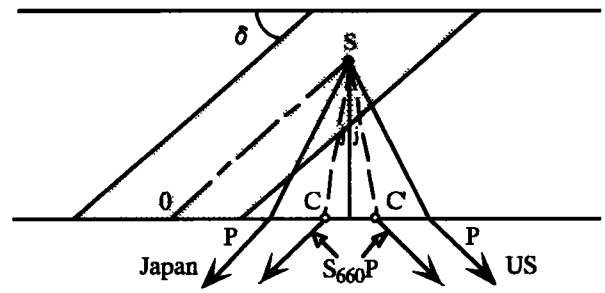

Fig. 2 Schematic illustration of a 2-D slab and ray paths of $S_{660}P$ directed towards Japan and California.

energy and indicate a phase arrival. On the basis of the N-th root stacking we can obtain the slowness (relative to that of the direct P wave) of a particular phase, which facilitates the correct identification of that phase. The $S_{660}P$ phase is characterized by a smaller value of slowness than that of the direct P-wave. The details of the stacking procedure are given by *Kawakatsu and Niu* [1994].

The travel-time difference between the direct P and the $S_{660}P$ phase ($\delta t_{S_{660}P-P}$) is then used to estimate the depth of the S-P conversion point at the 660-km discontinuity. To determine the travel-time difference, we cross-correlate P and $S_{660}P$ phases in stacked traces. We use the iasp91 seismic velocity model [*Kennett and Engdahl*, 1991] to convert the travel-time difference to the depth of the S-P conversion point. Assuming that all deep earthquakes occurred within the core of the slab, and that the dip of the slab is adequately constrained by deep seismicity, we also compute the horizontal distance between the slab core and the S-P conversion point using a 2-D slab model (Fig. 2). The fact that rays do not travel perpendicular to the strike direction of the slab is also taken into account when determining the conversion point. We adopt the slab model of *Fischer et al.* [1991], which consists of a straight slab within the northern section (dip 64°, strike 20°) and a more complex southern section consisting of a kinked slab that changes dip from 55° to 74° at depth 500 km and has a strike of 34°.

Results and Discussion

Analyzing the 29 events in the above manner produced a cross-section of S-P conversion-point positions. Fig. 3a shows the depth map of the 660-km discontinuity, and in Fig. 3b, the conversion-point depths are depicted as a function of horizontal distance from the slab core at a depth of 660 km. Closed circles in Fig. 3b represent conversion point depths obtained from the J-array data and open circles represent depths obtained from the California array data. Although some scattering is evident and may be attributed either to potential along-strike variation in the depth of the 660-km discontinuity or to the inadequate assumption that earthquakes occurs in the slab core, the trend that this discontinuity deepens as it nears the slab core is very clear. The greatest depth increase is about 70 km compared to the global average. The correction to a dipping

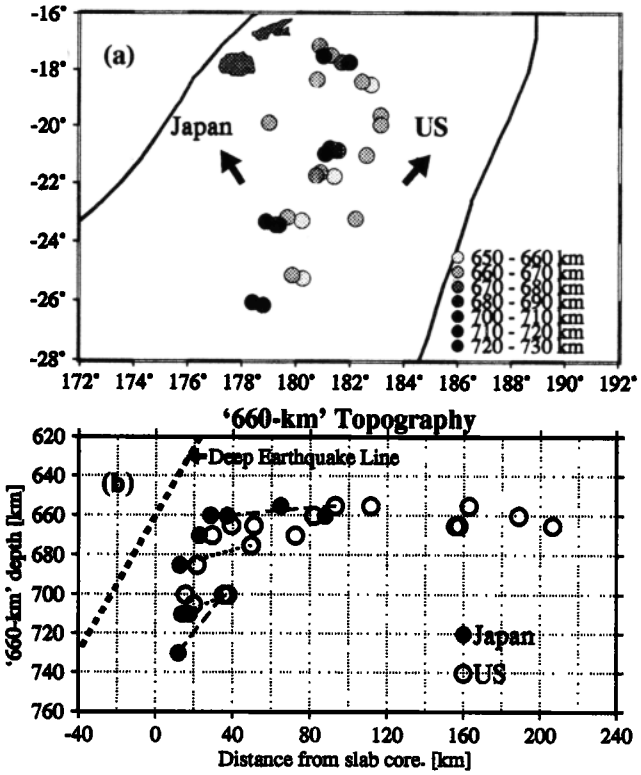

Fig. 3 *a)* Depth map of the '660-km' discontinuity. Great circle arc directions, which connect the epicentral region and the arrays, are shown by arrows. *b)* Depths of the '660-km' discontinuity are shown as a function of horizontal distance from the slab core. Closed circles represent conversion point depths obtained from the J-Array data, and open circles represent depths obtained from the California array data. Dotted line represents the deep seismic zone, which is assumed to be the slab core. Conversion-point pairs of the two events are connected by dashed lines. For conversion-point pairs of other two events with more complicated sources, dotted lines are used.

discontinuity merely requires that the conversion point location in Fig. 3b be shifted up and to the right by several kilometers.

Fig. 3b is obtained by projecting all the conversion points, which extend along the slab strike for nearly 1000 km, onto a single representative cross-section. The assumption of a 2-D slab geometry and the variation of the hypocentral position within the slab may distort the actual 3-D image of the 660-km discontinuity beneath the Tonga subduction zone.

Direct Comparison of Japan and US data. One method of direct examination of the undulation of the 660-km discontinuity is to compare the Japanese and Californian array data for the same event. Although S-P converted rays to both Japan and California initially travel almost directly downward, the S-P conversion points of rays directed toward Japan always lie closer to the slab than the conversion points of those directed toward California (Fig. 2). Depth discrepancies between these pairs of conversion points may reflect the undulation of the 660-km discontinuity across the slab. Among the nine events recorded by J-array since April 1991, only six were also recorded by the California array. Two of the six events exhibit clear $S_{660}P$ on the stacked traces of both the J-array and the California array data; a direct comparison is possible for these two events. Stacked traces with $S_{660}P$ slowness are plotted in Fig. 4a for both Japan and California. The arrival time of the $S_{660}P$ phase is indicated by a vertical line. To confirm the identification of $S_{660}P$, the stacked traces are compared with synthetic seismograms stacked in the same manner as the observed data (Fig. 4b). We calculate reflectivity synthetic seismograms [*Kennett*, 1988] using known focal mechanisms of the deep events [*Dziewonski et al.*, 1981] and the iasp91 model. The synthetic amplitude and polarity of $S_{660}P$ in the synthetic stacks are in good agreement with the stacks of the observed data, supporting our identification of $S_{660}P$. In the data (Fig. 4a), a delay of 1.0 to 3.0 sec between Japan and California arrivals is apparent. There are two more events for which we can observe a similar relative delay of $S_{660}P$ arrival in the J-array data. However, the source mechanisms of these two events are too complicated to give a convincing identification of $S_{660}P$.

In order to conclude that the conversion points of the Japan-directed rays lie deeper than those of California-directed rays, the possibility that the apparent $S_{660}P$ phase delay of J-array data is a consequence of the high seismic velocity slab must be eliminated. As shown in Fig. 2, the Japan-directed P-waves travel a considerable distance within the high velocity slab, which may result in a greater travel-time difference. To estimate the influence of the high-velocity slab on the travel-time difference between $S_{660}P$ and P arrivals observed at Japanese and Californian stations, we performed a 2-D ray tracing. We use a model with a straight slab having 100 km horizontal width and 60° dip. The seismic velocities within the slab are assumed to exceed those of the surrounding *iasp91* mantle by 5%. We consider two cases for the depth of slab penetration: (1) slab pene-

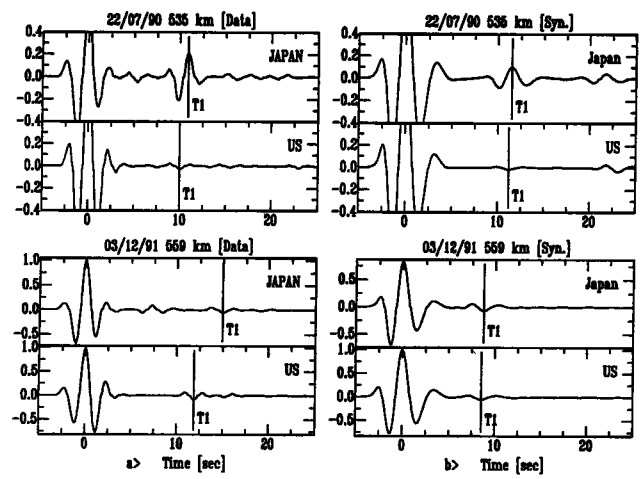

Fig. 4 *a)* Examples of two events that exhibit a clear $S_{660}P$ arrival (T1) on both J-Array and the California array stacked traces. For each event, stacked traces at the slowness of $S_{660}P$ are shown. The arrival time of the $S_{660}P$ phase is indicated by a vertical line. *b)* Synthetic stacked traces obtained through the same procedure as for the data.

tration terminating at a depth of 660 km; and (2) a slab penetrating to a depth of 850 km [*Fischer et al.*, 1991]. We find that the greatest discrepancy is no more than 0.4s, which occurs when the source is located on the lower border of the slab. For a 20 kilometer horizontal shift of the source within the slab core, the difference is at most 0.2s.

Since neither the ray paths directed to Japan nor those to California are in the downdip direction of the slab, we correct for the effect of the 3-D ray path in the following manner. Our first approximation is to assume that the ray path stays in the great circle plane which contains both the source and receiver. We further assume that the 2-D ray path is a projection of the 3-D ray path onto a plane perpendicular to the slab strike. Although neither of these approximations is justifiable in a strict sense, they may give a reasonable estimate of the 3-D effect when the departure from the 2-D situation is not so severe (i.e., Japan directed rays). Although the 3-D effect could be severe for the California directed rays, since ray paths to the California depart the slab soon (Fig. 2), they are less affected by the slab than those to Japan. We therefore think such 2D ray tracing can give a reasonable estimation of the travel-time anomaly introduced by the high velocity slab.

We assume that velocities of both P-wave (α) and S-wave (β) in the slab are 5% higher than those of the surrounding mantle; since $\beta < \alpha$, S-waves will have a larger travel-time anomaly than P-waves if they travel the same distance in the slab. On the other hand, as shown in Fig. 2, the direct P-wave travels almost parallel to the dip of the slab, while $S_{660}P$ has a much steeper take-off angle; the direct P-wave therefore travels a longer distance within the high-velocity slab than $S_{660}P$. The net effect is that the travel-time anomalies of both $S_{660}P$ and the direct P-wave are not much different. As a result, the high-velocity slab does not influence the travel-time difference $\delta t_{S_{660}P-P}$ significantly, although it does introduce as much as 1 sec travel-time anomaly to *each of* the P and the $S_{660}P$ waves [*Fischer et al.* 1991]. We therefore conclude that most of the 1.0 to 3.0 sec delay observed for $S_{660}P$ by J-array stations can be directly attributed to the differences in the depths of the conversion points.

Pairs of $S_{660}P$ conversion points estimated for each event are connected by broken lines in Fig. 3b. The fact that these pairs of points lie locally just beneath the corresponding earthquakes is direct evidence that the 660km discontinuity deepens as the conversion point nears the slab.

Accumulating this type of data, which can be obtained by combining data from seismic networks in different regions of the world, can help to "map" locally the depth variations of seismic discontinuities in the mantle. This in turn may be used to estimate to the temperature variations in the mantle. We are currently trying to compile a Japanese data set for the period before the operation of the J-array project (i.e., before 1990), so that the direct comparison of Japanese and Californian data can be made for a large number of events.

Acknowledgments. We are grateful to the J-array Data Center for supplying data. We also thank the data centers of the Southern California Seismographic Network and the regional network of the Earthquake Research Institute. We thank Dr. T. Iidaka for his assistance with the 2-D ray tracing programs. We wish to express our gratitude to Dr. J. Vidale for introducing the availability of the SCSN data. Finally, we thank Prof. Bob Geller, Drs. T. Iidaka and S. Mueller for critically reading the manuscript, and Drs. M. Weber and R. van der Hilst for constructive reviews.

References

Bock, G., and J. Ha, Short-period S-P conversion in the mantle at a depth near 700km, *Geophys. J. R. Astr. Soc.*, *77*, 593-615, 1984.

Dziewonski, A. M., T.-A. Chou, J. H. Woodhouse, Determination of earthquake source parameters from waveform data for studies of global and regional seismicity, *J. Geophys. Res.*, *86*, 2825-2852, 1981.

Fischer, K. M., K. C. Creager, T. H. Jordan, Mapping the Tonga slab, *J. Geophys. Res.*, *96*, 14403-14427, 1991.

Ito, E., and E. Takahashi, Postspinel transformations in system Mg_2SiO_4-Fe_2SiO_4 and some geophysical implication, *J. Geophys. Res.*,*94*, 10637-10646, 1989.

J-Array Group, The J-Array program: system and present status, *J. Geomag. Geoelectr.*, *45*, 1265-1274, 1993.

Kanasewich, E. R., *Time Sequence Analysis in Geophysics*, The University of Alberta Press, 364 pp, 1973.

Kawakatsu, H., and Niu F.-L., Evidence for a 920-km discontinuity in the mantle, *Nature*, *371*, 301-305, 1994.

Kennett, B. L. N., Systematic Approximations to the Seismic Wavefield, in *Seismological Algorithms*, edited by D. J. Doornbos, pp. 237-259, Academic Press, 1988.

Kennett, B. L. N., and E. R. Engdahl, Travel times for global earthquake location and phase identification, *Geophys. J. Int.*, *105*, 429-465, 1991.

Kincaid, C., and P. Olson, An experimental study of subduction and slab migration, *J. Geophys. Res.*, *92*, 13832-13840, 1987.

Mizuta, S., Y. Morita, H. Hamaguchi, 670km discontinuity beneath Fiji region (1), *Program and Abstracts, Seism. Soc. Japan*, *2*, 189, 1991 (in Japanese).

Richards, M. A., and C. W. Wicks Jr., S-P conversion from the transition zone beneath Tonga and the nature of the 670 km discontinuity, *Geophys. J. Int.*, *101*, 1-35, 1990.

Shearer, P. M., and T. G. Masters, Global mapping of topography on the 660 km discontinuity, *Nature*, *355*, 791-796, 1992.

Vidale, J. E., and H. M. Benz, Upper-mantle seismic discontinuities and the thermal structure of subduction zones, *Nature*, *356*, 678-682, 1992.

Wicks, C. W. Jr., and M. A. Richards, A detailed map of the 660-kilometer discontinuity beneath the Izu-Bonin subduction zone, *Science*, *261*, 1424-1427, 1993

Fenglin Niu and Hitoshi Kawakatsu,
Earthquake Research Institute, University of Tokyo
1-1-1 Yayoi, Bunkyo-ku, Tokyo 113, Japan.
(e-mail [niu,hitosi]@eri.u-tokyo.ac.jp)

(received September 7, 1994; revised December 1, 1994; accepted December 1, 1994.)